

Image potential and ion trajectories in secondary-ion mass spectrometry

R. A. Gibbs,* S. P. Holland,[†] K. E. Foley, B. J. Garrison, and N. Winograd

Department of Chemistry, The Pennsylvania State University, University Park, Pennsylvania 16802

(Received 24 August 1981)

The angle and energy distributions of Ni⁺ ions ejected from ion-bombarded Ni(001)*c*(2 × 2)-CO are shown to be in excellent agreement with classical trajectory calculations for Ni atoms if the calculations are corrected for the presence of an image force. Two important consequences of this observation are that the ionization probability R^+ is nearly isotropic and that it is only weakly dependent on particle velocity. These constraints impose severe restrictions on proposed ionization theories.

Ion desorption from solids is a general phenomenon which can be induced by photon, electron, or particle bombardment. The mechanism of ion formation has been well elucidated when the desorption is stimulated by photon¹ or electron fields,² although the processes which affect ionization during collisions between atoms in a solid remain quite speculative. This theoretical input is critically needed to interpret experimental results from a variety of ion-scattering experiments including secondary-ion mass spectrometry (SIMS). In this paper, we examine the ionization problem by performing the first detailed experimental measurements of the angular and energy distributions of ions ejected due to ion bombardment of a well-defined surface. As a model system we have chosen Ni(001)*c*(2 × 2)-CO bombarded by 1000-eV Ar⁺ at normal incidence since the original surface geometry of CO has been determined by low-energy electron diffraction³ and since the presence of CO enhances the observed Ni⁺ yield by more than 4 orders of magnitude over the clean Ni(001) surface.⁴ The results are in semiquantitative agreement with classical dynamical calculations of this system for the neutral particles if their trajectories are modified by the inclusion of an appropriate image force. This agreement provides a convincing basis for the classical dynamics model and suggests that the probability of ionization of the neutral atoms is isotropic and nearly independent of the ejected-particle velocity. The latter conclusion supports recent theoretical efforts aimed toward providing physical insight into the ionization process⁵ and indicates that Auger neutralization is not a dominant mechanism.

The angle-resolved SIMS measurements are performed using a specially designed UHV chamber such that the quadrupole mass filter (Riber AQX156) can be rotated with respect to the primary ion beam. This feature is achieved using a set of three 56-cm differentially pumped Teflon seals. A manipulator for the crystal then provides azimuthal rotation, heating to 1300 K, cooling to 175 K, and vertical translation to a LEED apparatus located on a different level

in the chamber. The secondary ions are then angle and energy selected using a 90° spherical electric sector in front of the mass analyzer. The calculated polar angle resolution, based on the size of the apertures and the field-free distance of the sample from the lens, is estimated to be ±7°. The azimuthal angle resolution $\Delta\phi$ can be approximated from the polar angle, θ , since $\Delta\phi \approx \Delta\theta/\sin\theta$. Using a zoom lens arrangement, the bandpass of the analyzer can be varied from approximately 2 eV for recording energy spectra to nearly 15 eV for obtaining maximum sensitivity. Details of the apparatus will be available elsewhere.⁶ The total ion flux during the experiment is kept below 10¹³ ions/cm² to avoid significantly altering the surface structure. The cut and polished Ni crystal was cleaned *in vacuo* in the standard fashion. The clean surface was then exposed to 2 L (1 L = 10⁻⁶ Torr sec) of CO to obtain a *c*(2 × 2) overlayer geometry.

The calculated energy and angular distributions were determined using a previously described classical dynamics procedure.⁷ The initial nuclear coordinates of the adsorbed CO were taken from LEED measurements.³ These results indicate that the CO is in a linear bonded site with the carbon atom 1.76 Å above the nickel atom. The exact form and parameters of the interaction potential have been published elsewhere.^{7,8} Comparison between the calculated distributions and the measured ones required the computation of approximately 1400 Ar⁺ ion impacts for both clean Ni(001) and Ni(001)*c*(2 × 2)-CO to obtain sufficient statistical accuracy.

It has generally been observed that energy distributions of ejected secondary ions are considerably broader than that of the neutrals. For example, for 1-keV Ar⁺ on Cu the ion energy distribution peaks at 4 eV and tails off as $E^{-0.5}$ while the neutral distribution peaks at 3 eV and tails off as roughly E^{-2} .⁹ Many explanations have been proposed to explain this effect, although most focus on the possibility that the primary phenomenon controlling the ionization probability is the Auger reneutralization rate. In

this case, the ionization probability R^+ is a function of ion velocity as¹⁰

$$R^+ \propto \exp(-A/a v_1), \quad (1)$$

where A is the Auger transition rate at the surface, a is a critical distance, and v_1 is the perpendicular velocity component of the ejecting ion. Values of A/a from 2.5×10^5 to 2×10^6 cm/sec have been reported.¹¹ On the other hand, a recent quantum-mechanical model of ionization predicts an R^+ which is only a weak function of v_1 .⁵

Our calculated energy distributions for Ni atoms ejected from Ni(001)_c(2×2)-CO are quite different from the rather broad energy distributions found experimentally for Ni⁺ ions as shown in Fig. 1. We can obtain reasonable agreement between calculated and experimental distributions at a polar angle of 30° by correcting the calculated trajectories using Eq. (1) and an A/a value of 1.1×10^6 cm/sec, although computed energy distributions at other angles then deviate rather dramatically from experimental curves. As we shall see later, this equation poorly predicts polar and azimuthal angle Ni⁺ ion intensities.

In contrast, incorporation of a simple image force allows quantitative agreement between the calculations of neutral atom trajectories and the experimentally measured ion distributions. To overcome the image force and escape the solid, the ion must perform work, E_{image} . If it is assumed that the particle instantaneously becomes an ion, E_{image} is given by

$$E_{\text{image}} = \frac{e^2}{4z} = \frac{3.6 \text{ eV}}{a_0}, \quad (2)$$

where a_0 is the height in angstroms of the particle above the jellium stepedge at the instant of ionization. If θ_n is the angle of the atom's velocity vector at this point, the ion emerges with a final direction given by

$$\theta_i = \tan^{-1} \left(\frac{E_0 \sin^2 \theta_n}{E_0 \cos^2 \theta_n - E_{\text{image}}} \right)^{1/2}, \quad (3)$$

where θ_i is the corrected polar ejection angle as measured from the surface normal of the leaving ion, and E_0 is the kinetic energy of the neutral particle ejected at polar angle θ_n . The corrected theoretical energy distribution using $E_{\text{image}} = 3.6$ eV is also shown in Fig. 1. The agreement with experiment over all polar angles is quite good. Note that in this comparison we choose a specific value of E_{image} without explicitly assuming the functional form given in Eq. (2).

A further test of the relevance of this correction can also be developed by comparing neutral and ionic trajectories of Ni at various polar and azimuthal angles. As shown in Fig. 2, a selection of both low- and high-kinetic-energy particles produces a maximum Ni⁺ signal at a polar angle of about 50°. The calculations produce a distribution similar in shape, which peaks at significantly lower angles. Correction of the neutral trajectories using Eq. (3) with $E_{\text{image}} = 3.6$ eV, however, provides quantitative agreement in both energy regimes. An E_{image} value other than 3.6 ± 0.3 eV yields a poor fit to the data in Figs. 1 and 2. It is also important to note that correction

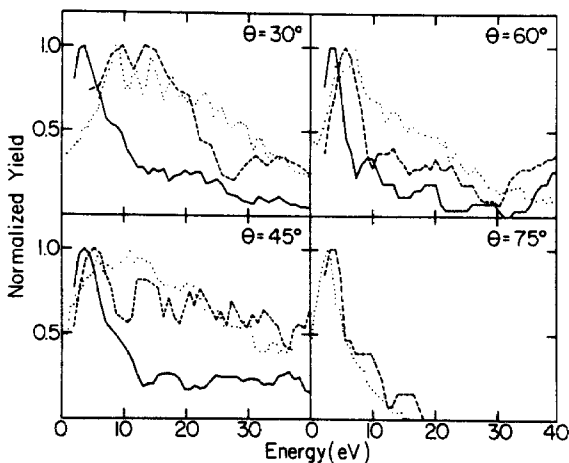


FIG. 1. Energy distributions for Ni ejected from Ni(001)_c(2×2)-CO due to bombardment by 1-keV Ar⁺ at normal incidence. The polar angle, θ , is defined with respect to the surface normal. The azimuthal angle, ϕ , is along the (100) direction for all cases. The three curves in each panel are identified as follows: — calculated Ni distribution, --- calculated Ni distribution with inclusion of the image force, and ··· experimental points for Ni⁺.

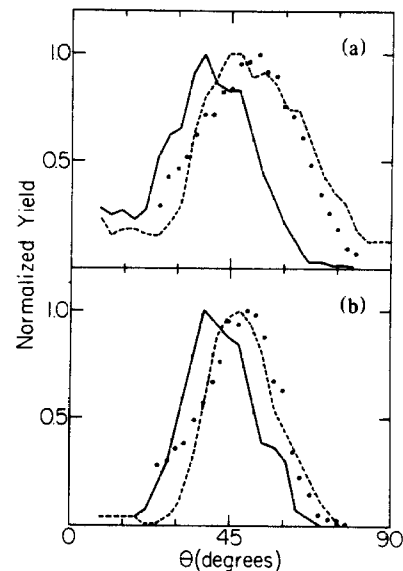


FIG. 2. Polar angle distributions for Ni ejected from Ni(001)_c(2×2)-CO. Experimental conditions and codings for each curve are the same as for Fig. 1. (a) The upper set of curves is recorded for a secondary ion energy of 7 ± 2 eV, while (b) the lower set of curves is taken at 22 ± 2 eV.

of the calculated trajectories using Eq. (1) shifts the polar distributions significantly closer to the normal than the experimental data.

Information contained in azimuthal angular spectra is more sensitive to surface structure than either the polar or energy distributions.^{12,13} The azimuthal spectra obtained at large polar angles should be strongly influenced by any image force, since the image force acts to bend particles originally ejected at smaller polar angles into the detector. In Fig. 3, the angular spectra obtained for 3 ± 3 -eV Ni⁺ ions ejected from Ni(001)*c*(2 × 2)-CO are shown at $\theta = 30^\circ$, 45° , 60° , and 70° . Predicted neutral and image force corrected distributions are also shown, again derived assuming the same E_{image} value of 3.6 eV. Although the magnitude of the measured anisotropy is slightly smaller than calculated at 45° and 30° , the level of agreement is quite remarkable. Note that the calculated distributions are unaffected by the incorporation of Eq. (1). It is of interest that if the CO is placed in other bonding geometries, that poor agreement with experiment is found. These types of angle-resolved experiments, then, should be valuable aids in the analysis of unknown surface structures.

It is clear that the classical dynamics calculations can provide an accurate description of ion trajectories with simple inclusion of an appropriate image force. The agreement between theory and experiment for Ni trajectories is excellent for energy distributions at various polar and azimuthal angles. Similar levels of agreement are found for Ni₂⁺ and NiCO⁺ trajectories, although statistical fluctuations in the theoretical development so far preclude detailed comparisons. Unfortunately, the CO⁺ ion is not experimentally observed.

If the above arguments concerning the presence of a relatively strong image force are correct, there are a number of constraints placed upon any ionization theory. First, the ion must be formed very close to the surface. The 1.0-Å distance we find for Ni(001)*c*(2 × 2)-CO should be viewed only qualitatively since other factors such as saturation of the image force¹⁴ and the change in partial charge on the ejecting atom with distance⁵ are not taken into account with our simple approach. A second constraint

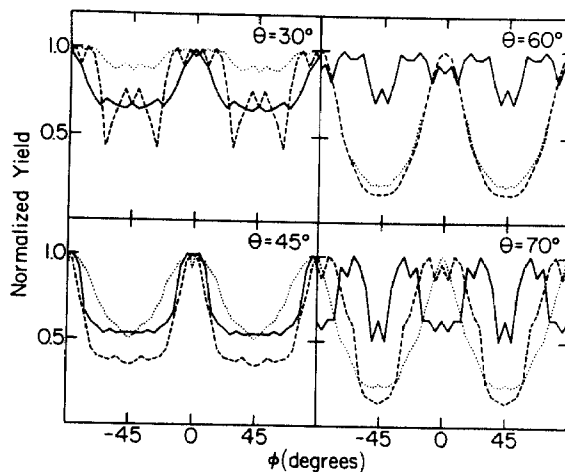


FIG. 3. Azimuthal angle distributions at various polar angles for Ni ejected from Ni(001)*c*(2 × 2)-CO. The curve codings are the same as for Fig. 1. Only those Ni particles with an energy of 3 ± 3 eV are detected. The value of $\phi = 0^\circ$ corresponds to $\langle 100 \rangle$, while $\phi = \pm 45^\circ$ corresponds to $\langle 110 \rangle$.

is that for Ni(001)*c*(2 × 2)-CO, R^+ is only weakly dependent on v_1 and is not a measurable function of ejection angle. These results have only recently been predicted using a quantum-mechanical model.⁵ This model utilizes the electronic density of states to calculate electronic hopping probabilities during the atomic collisions which lead to particle ejection. Although the influence of ejection angle on R^+ has not been fully tested, it is possible that the large number of different ejection mechanisms which are observed cause an averaging of angular anisotropies. At least for Ni(001)*c*(2 × 2)-CO, the Auger neutralization mechanism does not appear to be important.

The authors wish to thank the National Science Foundation, The Office of Naval Research, The Air Force Office of Scientific Research, and the Petroleum Research Foundation administered by The American Chemical Society for financial support. One of us (B.J.G.) also acknowledges receipt of an A. P. Sloan Foundation Research Fellowship and a Camille and Henry Dreyfus Foundation grant.

*Present address: Westhollow Research Center, Shell Development Company, Houston, Tex. 77001.

¹Present address: IBM, General Technology Division, Essex Junction, Vt. 05452.

¹M. L. Knotek, V. O. Jones, and V. Rehn, Phys. Rev. Lett. **43**, 300 (1979).

²M. L. Knotek and P. J. Feibelman, Phys. Rev. Lett. **40**, 964 (1978); D. Menzel and R. Gomer, J. Chem. Phys. **41**, 311 (1964); P. A. Redhead, Can. J. Phys. **42**, 886 (1964).

³M. Passler, A. Ignatiev, F. Jona, D. W. Jepsen, and D. M.

Marcus, Phys. Rev. Lett. **43**, 360 (1979); S. Andersson and J. B. Pendry, *ibid.* **43**, 363 (1979).

⁴P. H. Dawson and W. Tam, Surf. Sci. **91**, 153 (1980).

⁵Z. Šroubek, K. Ždánký, and J. Žavadil, Phys. Rev. Lett. **45**, 580 (1980).

⁶R. A. Gibbs and N. Winograd, Rev. Sci. Instrum. **52**, 1148 (1981).

⁷N. Winograd, B. J. Garrison, and D. E. Harrison, Jr., J. Chem. Phys. **73**, 3473 (1980).

⁸D. E. Harrison, Jr., P. W. Kelly, B. J. Garrison, and N.

Winograd, Surf. Sci. 76, 311 (1978).

⁹R. G. Hart and C. B. Cooper, Surf. Sci. 94, 105 (1980).

¹⁰H. D. Hagstrum, J. Vac. Sci. Technol. 12, 7 (1975).

¹¹K. Wittmaack, in *Inelastic Ion-Surface Collisions*, edited by N. H. Tolk, J. C. Tully, W. Heiland, and C. W. White (Academic, New York, 1977), p. 153.

¹²S. P. Holland, B. J. Garrison, and N. Winograd, Phys. Rev. Lett. 43, 220 (1979); 44, 3473 (1980).

¹³N. Winograd and B. J. Garrison, Acc. Chem. Res. 13, 406 (1980).

¹⁴R. E. Dietz, E. G. McRae, and R. L. Campbell, Phys. Rev. Lett. 45, 1280 (1980).